GEOPHYSICAL RESEARCH LETTERS, VOL. 24, NO. 6, PAGES 667-670, MARCH 15, 1997

# Climate forcing-response relationships for greenhouse and shortwave radiative perturbations

V. Ramaswamy

NOAA Geophysical Fluid Dynamics Laboratory, Princeton, New Jersey

C-T. Chen

Department of Earth Sciences, National Taiwan Normal University, Taipei, Taiwan

**Abstract.** The earth's climate system is subject to radiative forcings caused by perturbations in the infrared 'greenhouse' effect and absorbed solar energy. The forcings can be classified as being global in extent (e.g., increase of $CO_2$) or spatially confined to the northern hemisphere midlatitudes (e.g., anthropogenic sulfate aerosols). Of central importance to climate change assessments are the characteristics of the global and latitudinal changes, and the forcing-response relationships for different kinds of perturbations. Using a general circulation climate model with fixed cloud distributions and microphysical properties, we analyze the equilibrium climate responses to different perturbations representing global and spatially localized radiative forcings. The total climate feedback in the various experiments does not differ significantly, and the global-mean climate sensitivity (ratio of the equilibrium global-mean surface temperature change to the global-mean imposed radiative forcing) behaves in a near-invariant manner for both global and spatially confined forcings. However, relative to the global perturbation cases, forcings confined to the northern hemisphere midlatitudes exhibit a steepening of the meridional gradient of the temperature response in that hemisphere.

## 1. Introduction

Increases in the concentrations of well-mixed 'greenhouse' gases like $CO_2$ cause a global increase in the infrared radiative energy trapped by the Earth's surface-atmosphere system (positive radiative forcing). In contrast, the anthropogenic increase of sulfate aerosols over the northern hemisphere midlatitudes is presumed to cause an increase in the local solar reflectance or albedo (equivalently, decrease in the absorbed solar energy), yielding a negative forcing [*Schimel et al.*, 1996]. This spatially confined shortwave forcing differs from the global-scale forcing due to, for example, changes in the solar constant [*Manabe and Wetherald*, 1980; *Hansen et al.*, 1984], or a possible worldwide change in the albedo of the surface-atmosphere system [e.g., *Ramaswamy and Chen*, 1993]. A crucial issue in climate change is the degree to which the modeled forcing-response relationships for these different perturbations are similar or dissimilar, including the aspect of amplification of the response by the feedbacks in the climate system. A related point is the usefulness of the global-mean forcing in gaging the relative climate impacts due to various types of radiative perturbations. The outcome is particularly important for ascertaining the agreement or contrast in the climate effects between global-scale and spatially localized radiative forcings.



Paper number 97GL00253.

## 2. Climate Model and Forcing Experiments

We address the problem by examining the equilibrium climate responses of a general circulation model (GCM) to different kinds of imposed radiative forcings. The GCM employed follows, with some modifications, an earlier Geophysical Fluid Dynamics Laboratory atmospheric model (resolution: 4.5°latitude, 7.5° longitude, 9 levels) with fixed low, middle and high cloud amounts (i.e., the Fixed Cloud model of *Manabe and Broccoli*, 1985). It is coupled to a static, isothermal mixed-layer ocean 50 meters deep with prescribed ocean heat fluxes [*Chen and Ramaswamy*, 1996a; hereafter CR96a]. The process of sea-ice formation and changes are explicitly incorporated. The model includes an explicit representation of the cloud solar radiative properties in terms of liquid water path (LWP) and effective drop radius ($r_e$) [*Chen and Ramaswamy*, 1995; hereafter CR95]. The model's simulation of present-day climate, while not quantitatively perfect, is in reasonable qualitative agreement with observations (CR96a). In the perturbation experiments described below, cloud microphysical properties, their geographical and altitude locations, and amounts are held fixed throughout each integration.

Seven perturbation experiments ('A' to 'G') are performed (Table 1), with the forcing ($\Delta R$) in 'A' to 'D' global in extent, while being spatially confined in 'E', 'F' and 'G'. The labels 'A' to 'D' correspond, respectively, to the $2xCO_2$, GLD, GLI, GLI/2 experiments described in CR96a, while 'E' and 'F' correspond to the LLI and LCM experiments discussed in *Chen and Ramaswamy* [1996b; hereafter CR96b]. Experiment 'A' is a doubling of the model's atmospheric carbon dioxide concentration (greenhouse forcing) and is similar in essence to many earlier experiments with the present and other models.

Experiments 'B' to 'F' represent different shortwave forcings, each initiated in the model by perturbing the net solar energy absorbed. Shortwave forcings can occur due to a change in the insolation [*Manabe and Wetherald*, 1980], or by the alteration of the amount of sunlight reflected (i.e., albedo) by the surface and atmospheric constituents [*Mitchell et al.*, 1995; CR95]. For the present modeling purposes, we simulate shortwave forcings by perturbing the albedo of the model's low clouds (height < 3 km.; cf. *Erickson et al.*, 1995). Since the low cloud albedo is a function of cloud optical depth which, in turn, depends on the ratio LWP/ $r_e$ [*Slingo*, 1989], the shortwave forcings at the tropopause (approximately the same as at the top-of-the-atmosphere) are obtained (Table 1)

**Table 1.** Global-mean forcing (ΔR (Global)), surface temperature change $\Delta T_s$ (Global) and climate sensitivity $G_f$ = [$\Delta T_s$ (Global)/ ΔR (Global)] for greenhouse and albedo perturbation experiments. Albedo forcings (changes in absorbed shortwave energy) are obtained by imposing uniform fractional changes in the low cloud microphysical properties (liquid water path, LWP, or effective drop radius, $r_e$) throughout the considered domain, while the greenhouse forcing is obtained by a doubling of $CO_2$. The forcing here is quantified by the *adjusted* global-mean net radiative flux change at the tropopause [*Shine et al., 1995*]. Unit for forcing is Watts per square meter and for temperature in degrees Kelvin.

| Experiment | Imposed perturbation | ΔR (Global) ($W m^{-2}$) | $\Delta T_s$ (Global) (K) | $G_f$ ($K/W m^{-2}$) |
|---|---|---|---|---|
| Greenhouse Change (Global) | | | | |
| A | 2 x $CO_2$ | +3.66* | +2.48 | 0.68 |
| Albedo Change (Global) | | | | |
| B | LWP decrease by 25% | +3.62 | +2.50 | 0.69 |
| C | LWP increase by 37% | -3.63 | -2.79 | 0.76 |
| D | LWP increase by 17% | -1.86 | -1.37 | 0.74 |
| Albedo Change (Local); 20-70N | | | | |
| E | LWP increase by 100% | - 1.87 | -1.39 | 0.74 |
| F (Land) | $r_e$ decrease by 28% | -0.81 | -0.63 | 0.78 |
| G (Eurasia) | $r_e$ decrease by 50% | -1.09 | -0.78 | 0.71 |

* The *adjusted* global-mean forcing for $CO_2$ doubling (i.e., after stratospheric temperature equilibration) is estimated in an approximate manner (CR96a); it is less than the *instantaneous* forcing by ~6%. For the shortwave perturbation experiments ('B' to 'G'), there is no ambiguity between *instantaneous* and *adjusted* forcings owing to negligible perturbations in the globally-averaged stratospheric temperatures.

by imposing fractional changes in LWP or $r_e$ (CR96a,b). Because the model's cloud distributions are fixed, such perturbations constitute steady atmospheric solar radiative forcings. The longwave component due to the perturbations is negligible and thus ignored.

Experiment 'B' has a similar global-mean forcing as 'A', but results from a decrease of the planetary albedo caused by an imposed decrease in the low cloud liquid water path (Table 1). In 'C', the low cloud albedo is increased such that the global-mean forcing has the same value as in 'A' and 'B', but with an opposite sign. The value in 'D' is about one-half of that in 'C'. The forcings in 'B', 'C', and 'D' yield a ~1-2% change in the solar energy absorbed by the planet.

Experiments 'E' and 'F' consist of an albedo increase in the northern hemisphere midlatitude (20-70N) regions, with the domain for 'F' including only the land areas. Experiment 'G' further confines the forcing to the Eurasian region in the model (longitudes 5E to 100E). The global-mean forcing in 'E' is similar to 'D' and more than twice that of 'F' while experiment 'G' has a global-mean forcing of -1.1 $W/m^2$, about 34% larger than 'F'. While the precise value of the forcings chosen is not critical for this sensitivity investigation, it is worth noting that the numbers for 'E', 'F' and 'G' are approximately within the estimates for present and future total anthropogenic sulfate aerosol forcings [*Schimel et al.*, 1996], with the idealized domains here roughly typical of the northern hemisphere regions where the major perturbations are presumed to occur. In an overall sense, the suite of experiments here fall into three separate categories of radiative forcings (Table 1).

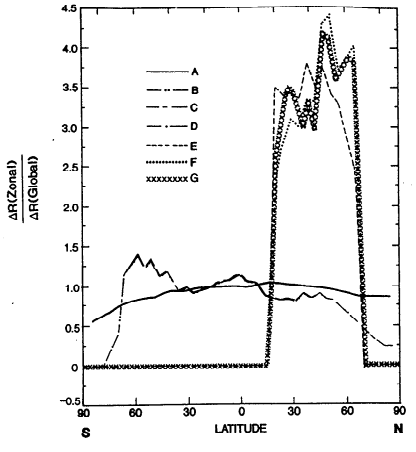


**Figure 1.** Spatial distribution of the initial zonal-mean radiative forcing, relative to the global-mean value, for each of the perturbation experiments. A: doubling of $CO_2$; B, C and D: global changes in the solar energy absorbed; E: change in the solar energy absorbed in the 20-70 N belt; F: same as E, except over land areas only; G: same as E, except over the Eurasian region (5E to 100E) only. See text for details.

To analyze the relative spatial pattern of the forcings, we perform a normalization viz., divide the zonal-mean values for each forcing by the global-mean (Figure 1). All the global albedo experiments ('B', 'C', 'D') have a similar distribution, with the cloud amounts in the southern hemisphere midlatitudes accounting for a larger forcing there [*Ramaswamy and Chen*, 1993]. For the sake of comparison with the spatial pattern of the albedo forcings, the pattern for $CO_2$ doubling is also shown. [Note: the $CO_2$ - induced zonal forcing employed here is the "instantaneous" value; this differs slightly from that obtained after considering an equilibration in the thermal state of the stratosphere - the so-called "adjusted" forcing (*Shine et al.*, 1995); however, the zonal patterns are nearly the same for both the "instantantaneous" and "adjusted" forcings (*WMO*, 1986)]. There is a considerable difference between the patterns of 'B', 'C' and 'D', and those of the spatially confined experiments 'E', 'F' and 'G', particularly in the northern hemisphere midlatitudes. The patterns for the northern hemisphere albedo change experiments differ significantly from that for increase in $CO_2$ ('A'). Thus, different forcings can have the same global-mean, but arrived at through significantly different spatial distributions.

For each perturbation 'A' to 'G', the model is integrated to a new equilibrium state, which is the climate response to that forcing. The integration period in each simulation is long enough (35 years) to ensure an equilibrated state for the present model, with the average of the surface temperature ($\Delta T_s$) over the last 10 years representing the equilibrium response. The perturbations can be regarded as external forcings

that induce changes in the internal variables of the surface-atmosphere system (water vapor, surface albedo, lapse rate), thus leading to feedbacks [*Wetherald and Manabe*, 1988].

## 3. Climate Responses

The global climate sensitivity $G_f$ is defined as the ratio of the global-mean equilibrium surface temperature change to the "adjusted" global-mean tropopause radiative forcing [*Shine et al.*, 1990], where "adjusted" implies allowing for the equilibration of the global-mean stratospheric temperature in response to the perturbation. This adjustment is of importance only for the $2xCO_2$ perturbation while being negligible for the present shortwave perturbation experiments. For the $2xCO_2$ perturbation, the global-mean "adjusted" forcing is computed according to the method in CR96a. $G_f$ is found to be approximately similar (Table 1; within 15%) and not significantly different for the various forcings - global-scale or spatially confined. The global-mean response is thus relatively insensitive to the spatial pattern of the forcing. $G_f$ (Table 1) is more than twice the value without any feedbacks (~0.3 K/ ($Wm^{-2}$)) [*Wetherald and Manabe*, 1988; CR96a], testifying to the significant role of the feedbacks in determining the climate response for any kind of perturbation. The values of $G_f$ also imply that the total global feedback effect due to changes in temperature, lapse-rate, water vapor and surface albedo is about the same for all forcings. The closeness of $G_f$ in experiments 'A', 'B' and 'C' reaffirms earlier results that have compared solar irradiance and $2xCO_2$ perturbations [*Manabe and Wetherald*, 1980; *Hansen et al.*, 1984]. The approximate similarity of $G_f$ for albedo and greenhouse forcings is consistent with other GCM studies, including those with localized forcings [*Marshall et al.*, 1994; *Penner et al.*, 1996; *Cox et al.*, 1995]. It may be noted that all the studies, including the present, have dealt with small values of forcing (<4 $W/m^2$; as reference, the global absorbed solar flux is ~240 $W/m^2$). Considering all the cases and within the parameter range studied here, it can be inferred that, whether it is a greenhouse, or global or spatially confined northern hemisphere albedo forcing, a reasonable estimate of the global-mean surface temperature response can be derived directly using the global-mean forcing and the model climate sensitivity $G_f$. It also does not matter much whether the initial forcing is mainly at the surface (as in the shortwave experiments 'B' to 'F'), or distributed between troposphere and surface (infrared greenhouse forcing; experiment 'A'). Although $G_f$ exhibits a near-invariant quality, note that its actual value can be expected to depend on the parameterization of the various physical processes, and thus may be expected to differ from one GCM to another.

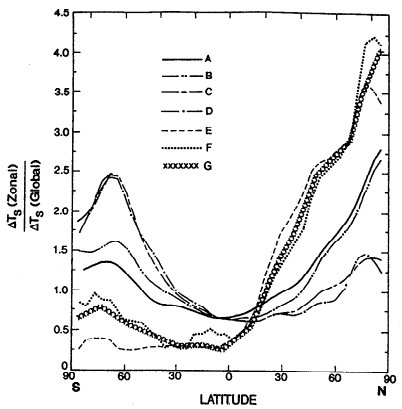


**Figure 2.** Spatial distribution of the zonal-mean surface temperature change, relative to the global-mean value, for each of the perturbation experiments A to G. See Table 1 and caption of Figure 1 for a description of the experiments.

To obtain perspectives into the spatial distribution of the responses to the different forcings, we plot the normalized zonal response pattern in Figure 2. This is obtained by dividing the zonal-mean surface temperature change by the global-mean. A nonuniform spatial pattern arises for each experiment which differs markedly from the corresponding pattern for the forcing (Figure 1), with an amplification in the polar regions. This is attributable to a significant role of the feedbacks which, as already indicated, strongly influence the global climate sensitivity. Although the global-mean change has about the same magnitude for the positive ('A' and 'B') and negative ('C' and 'D') global-scale forcings (Table 1), there is a difference in the spatial distribution of the response for these two types of forcings in the high latitudes. As explained in CR96a, this is attributable to differences in the magnitude of the changes occurring in the model's sea-ice extent and thickness for positive and negative forcings, which leads to differences in the ice-albedo feedback and the temperature response. These high latitude differences, it is cautioned, could be an artifact of the fixed clouds assumption in the present study. Further, it is noted that the responses at polar latitudes are subject to a high degree of variability [*Manabe and Stouffer*, 1996].

In contrast to the patterns for 'A' to 'D', 'E', 'F' and 'G' exhibit relatively stronger responses near and poleward of the northern hemisphere midlatitudes. Note, however, that these cases exhibit an apparent response in the southern hemisphere even though there is no initial forcing imposed there, in accord with the results of *Taylor and Penner* [1994]. The presence of a dominant signal in the mid-to-high latitudes for 'E', 'F' and 'G' resembles results seen in other simulations of northern hemisphere midlatitude albedo perturbations [*Taylor and Penner*, 1994; *Mitchell et al.*, 1995; *Cox et al.*, 1995]. Figure 2 illustrates that, even if the global-mean temperature change is the same for the various forcings, the meridional gradient of the surface temperature change could be different. Specifically, the spatially localized forcings yield a steeper equator-to-pole temperature change pattern in the northern hemisphere relative to the global-scale perturbations. By contrast, in the southern hemisphere, due to the absence of a forcing in that hemisphere and given the model's weak interhemispheric exchange (CR96b), 'E', 'F' and 'G' have a less sharp meridional structure than do 'A', 'B', 'C', and 'D'. The difference in the response characteristics of global and spatially confined forcings is similar to the *Manabe and Broccoli* (1985) study which investigated the impacts of expanded ice sheets lying primarily in the Northern Hemisphere.

## 4. Discussion

The results here are of particular relevance for the newly emergent climate forcing-response questions in the context of radiative perturbations that are not globally distributed like the greenhouse gas forcing or solar constant changes. An example of this is the tropospheric sulfate aerosols arising due to anthropogenic means [*Schimel et al.*, 1996]. On the one hand, the global climate sensitivity is approximately similar not only for $2xCO_2$ and global albedo perturbations, but also for shortwave forcings that span a less-than-global extent - down to midlatitude and even to continental spatial scales in the northern hemisphere. For greenhouse and albedo perturbations over such domains, the global-mean radiative forcing can be regarded as a useful, simple basis for estimating the global-mean surface temperature response. But, on the other hand, the differences in the spatial pattern of changes between

the global and non-global forcings (Figure 2) bear an equally important implication; viz., there is a restriction in the significance of contrasts drawn between different perturbations based merely on global-mean forcing (or response). Forcings confined to the northern hemisphere tend to yield a steepening of the normalized meridional temperature gradient in that hemisphere, which is in sharp contrast to the effects due to global-scale forcings, positive or negative. Thus, global-mean forcings cannot be used readily to distinguish between the regional climate effects of global-scale and spatially localized perturbations.

The contrasts in the meridional distribution of temperature change between the global and local forcings raise the possibility of contrasts in the atmospheric dynamical responses, and in the asymmetrical nature of changes between the two hemispheres. This would further weaken the validity of assessing climatic impacts solely on the basis of global-mean quantities; e.g., from CR96b, it is evident that the spatially localized forcing cases yield distinct precipitation responses in the northern and southern tropical regions that is not found for the globally extent forcing cases.

An uncertainty in the present calculations relates to the still poorly defined role of cloud feedback mechanisms. The fixed-clouds assumption employed here could be suppressing some important cloud-related feedbacks that affect both the zonal- and global-mean responses. Other modeling uncertainties concern the accuracy in the representations of various physical processes (e.g., convection) and absence of a dynamically interactive ocean. It is likely, however, that the basic finding here concerning the existence of contrasts in the meridional surface temperature response to global and local forcings will be unaffected by the uncertainties, thus extending the findings of *Santer et al.* [1995] and *Cox et al.* [1995].

The nature of the greenhouse perturbation examined here is typical of the important trace gases, but differs from that of tropospheric ozone [*Hansen et al.*, 1996]. Also, transient forcings (e.g., volcanic aerosols) have not been considered in this climate sensitivity study. In view of the increasing climatic importance of radiative perturbations that are neither global in scale nor spatially homogeneous, particularly tropospheric species [*Schimel et al.*, 1996], further model studies are needed to explore the responses to forcings with varying spatial (including vertical) inhomogeneities [e.g., *Hansen et al.*, 1996]. This would enable a generalization of the global and regional climate sensitivities for the diverse radiative forcings acting on the climate system - global and local, greenhouse and shortwave.

**Acknowledgments.** The authors are grateful to A. Broccoli, L. Donner and T. Wigley for their constructive and valuable comments and suggestions.

## References

Chen, C-T., and Ramaswamy, V., Parameterization of the solar radiative characteristics of low clouds and studies with a general circulation model, *J. Geophys. Res.*, *100*, 11611-11621, 1995.

Chen, C-T., and V. Ramswamy, Sensitivity of simulated global climate to perturbations in low cloud microphysical properties. I. Globally uniform perturbations, *J. Climate*, *9*, 1385-1402, 1996.

Chen, C-T., and V. Ramaswamy, Sensitivity of simulated global climate to perturbations in low cloud microphysical properties, II. Spatially localized perturbations, *J. Climate*, 9, 2788-2801, 1996.

Cox, S. J., W-C. Wang and S. E. Schwartz, Climate response to forcings by sulfate aerosols and greenhouse gases, *Geophys. Res. Lett.*, *18*, 2509-2512, 1995.

Erickson, D. J., R. J. Oglesby, and S. Marshall, Climate response to indirect anthropogenic sulfate forcing, *Geophys. Res. Lett.*, *22*, 2017-2020, 1995.

Hansen, J., et al., in *Climate Processes and Climate Sensitivity*, Geophys. Monogr. Ser., *29*, 130-263, 1984.

Hansen, J., M. Sato and R. Ruedy, Radiative forcing and climate response, submitted to *J. Geophys. Res.*, 1996.

Manabe, S., and Broccoli, A. J., A comparison of climate model sensitivity with data from the last glacial maximum, *J. Atmos. Sci.*, *42*, 2643-2651, 1985.

Manabe, S., and R. J. Stouffer, Low-frequency variability of surface air temperature in a 1000-year integration of a coupled atmosphere-ocean-land surface model, *J. Climate*, 9, 376-393, 1996.

Manabe, S., and Wetherald, R., On the distribution of climate change resulting from an increase in $CO_2$ content of the atmosphere, *J. Atmos. Sci.*, *37*, 99-118, 1980.

Marshall, S. E., R. J. Oglesby, J. W. Larson and B. Saltzmann, A comparison of GCM sensitivity to changes in $CO_2$ and solar luminosity, *Geophys. Res. Lett.*, *21*, 2487-249, 1994.

Mitchell, J. F. B., T. J. Johns, J. M. Gregory and S. F. B. Tett, Climate response to increasing levels of greenhouse gases and sulfate aerosols, *Nature*, *376*, 501-504, 1995.

Penner, J. E., T. M. L. Wigley, P. Jaumann, B. D. Santer, and K. E. Taylor, Anthropogenic aerosols and climate change: A method for calibrating forcing. Submitted to *Assessing Climate Change-The Story of the Model Evaluation Consortium for Climate Assessment*, in press, 1996.

Ramaswamy, V., and Chen, C-T., An investigation of the global solar radiative forcing due to changes in the cloud liquid water path, *J. Geophys. Res.*, *98*, 16703-16712, 1993.

Santer, B. D., K. E. Taylor, T. M. L. Wigley, J. E. Penner, P. D. Jones and U. Cubasch, Towards the detection and attribution of an anthropogenic effect on climate, *Clim. Dyn.*, *12*, 77-100, 1995.

Schimel, D. et al., Radiative forcing of climate change, in *Climate Change 1995: The Science of Climate Change, Contribution of Working Group I to the Second Assessment of the Intergovernmental Panel on Climate Change* (J. T. Houghton et al., eds.), Cambridge University Press, New York, pp 65-131, 1996.

Shine, K. P., Y. Fouquart, V. Ramaswamy, S. Solomon and J. Srinivasan, Radiative Forcing, in *Climate Change 1994: Radiative Forcing of Climate Change and An Evaluation of the IPCC IS92 Emission Scenarios* (J. T. Houghton et al., eds.), Cambridge University Press, Cambridge, New York, pp. 163-203, 1995.

Slingo, A., A GCM parameterization of the shortwave radiative properties of water clouds, *J. Atmos. Sci.*, *46*, 1419-1427, 1989.

Taylor, K. E., and J. E. Penner, Response of the climate system to atmospheric aerosols and greenhouse gases, *Nature*, *369*, 734-737, 1994.

Wetherald, R. T., and S. Manabe, Cloud feedback processes in a general circulation model, *J. Atmos. Sci.*, *45*, 1397-1415, 1988

WMO, *Atmospheric Ozone 1985, Global Ozone Research and Monitoring Project Report No. 16*, World Meteorological Organization, Geneva, Chapter 15, 1986.

---

V. Ramaswamy, NOAA Geophysical Fluid Dynamics Laboratory, P.O. Box 308, Princeton, NJ 08542. (e-mail: vr@gfdl.gov)

C-T. Chen, Department of Earth Sciences, National Taiwan Normal University, Taipei, Taiwan. (e-mail: chen@cloud.geos.ntnu.edu.tw)

(Received September 26, 1996; revised January 22, 1997; accepted January 27, 1997.)